Manufacturing Letters 32 (2022) 100–103

Contents lists available at ScienceDirect

Manufacturing Letters

journal homepage: www.elsevier.com/locate/mfglet

Letters

High temperature nanoindentation behavior of additively and traditionally manufactured Inconel 625

Majid Vaseghi [a], Ali Tajyar [a], Fariborz Tavangarian [b], Ali Beheshti [c,*], Keivan Davami [a,*]

[a] Department of Mechanical Engineering, University of Alabama, Tuscaloosa, AL, USA
[b] Mechanical Engineering Program, School of Science, Engineering and Technology, Pennsylvania State University, Middletown, Harrisburg, PA, USA
[c] Department of Mechanical Engineering, George Mason University, Fairfax, VA 22030, USA

ARTICLE INFO

Article history:
Received 17 January 2022
Received in revised form 5 May 2022
Accepted 21 May 2022
Available online 28 May 2022

Keywords:
IN 625
High Temperatures
Additive Manufacturing
Nanoindentation
Creep Behavior

ABSTRACT

Additively manufactured (AM) nickel-based superalloys, such as Inconel 625 (IN 625), are promising candidates for complex systems with high operating temperatures. In this work, an analysis was conducted to extract material properties such as hardness, elastic modulus, and creep properties of both AM IN 625 and traditionally manufactured (TM) IN 625 after annealing through an instrumented nanoindentation technique from room temperature up to 700 °C. The results for both specimens were compared and indicated that creep deformation decreases with the temperature increase up to 500 °C where no creep was observed for the AM IN 625 specimens at 500 °C.

1. Introduction

IN 625 superalloy is generally used in harsh environments where it needs to withstand not only high temperatures but also elevated stress during operations. Attributes such as excellent mechanical strength, creep strength, and remarkable protection against corrosion as well as oxidation make the alloy an ideal choice for harsh environments. Although IN 625 is a predominantly solid solution strengthened, strengthening precipitates also contribute to its high temperature stability and strength. When the material is aged at 680–870 °C, the formation of γ” precipitates such as fine Ni_3Nb, Ni_3Ti, and Ni_3Al type precipitates majorly affects the material behavior [1].

3D printing technique of direct metal laser sintering (DMLS) has recently emerged as a successful manufacturing process to fabricate complex metallic parts, in particular, superalloys [2]. Phenomena that inherently exist in the DMLS process, such as laser-powder-melt pool interactions, fast cooling, and high temperature gradient, significantly affect the mechanical properties of AM parts [3,4] including those of IN 625 [5]. The porosity, columnar grain structure, and compositional inhomogeneity of AM superalloys add complexity to the interpretation of their material behavior and modeling, in particular, under creep deformation. Several experimental and numerical studies have been performed to optimize the process parameters in order to fabricate high-quality IN 625 with desirable mechanical properties [5–7]. For instance, Ning et al. emphasized the effects of temperature distribution on the mechanical properties and dimensional accuracy of the AM parts [5]. They developed an analytical model for temperature prediction of single-track scan and multi-track scans considering scanning strategy [5]. Wu et al. [8] developed a microstructure-based creep model for AM nickel-based superalloys that took into account the relationship between the cavity formation kinetics and creep deformation. Recently, Son et al. [9] conducted high temperature uniaxial (macroscale) creep tests for AM IN 625 alloys built through DMLS process at various stresses for 650–800 °C. They found that AM IN 625 has equal or superior creep strength at 650–800 °C compared to its wrought counterpart.

The high temperature nanoindentation technique is an effective and versatile method to evaluate the nano/micro-scale material properties such as elastic modulus, hardness, and creep behavior at elevated temperatures [10]. Elevated temperature mechanical properties of nickel-based superalloys IN 617 and its oxide layer as well as mechanical and creep properties of IN 718 have been recently investigated through instrumented nanoindentation [11–14]. Recently, AM IN 625 elastic modulus and hardness (up to 510 °C) were investigated through nanoindentation [15]. Recent reports show that the creep behavior of AM IN 625 is generally dif-

* Corresponding authors.
E-mail addresses: abehesh@gmu.edu (A. Beheshti), kdavami@eng.ua.edu (K. Davami).

https://doi.org/10.1016/j.mfglet.2022.05.001
2213-8463/

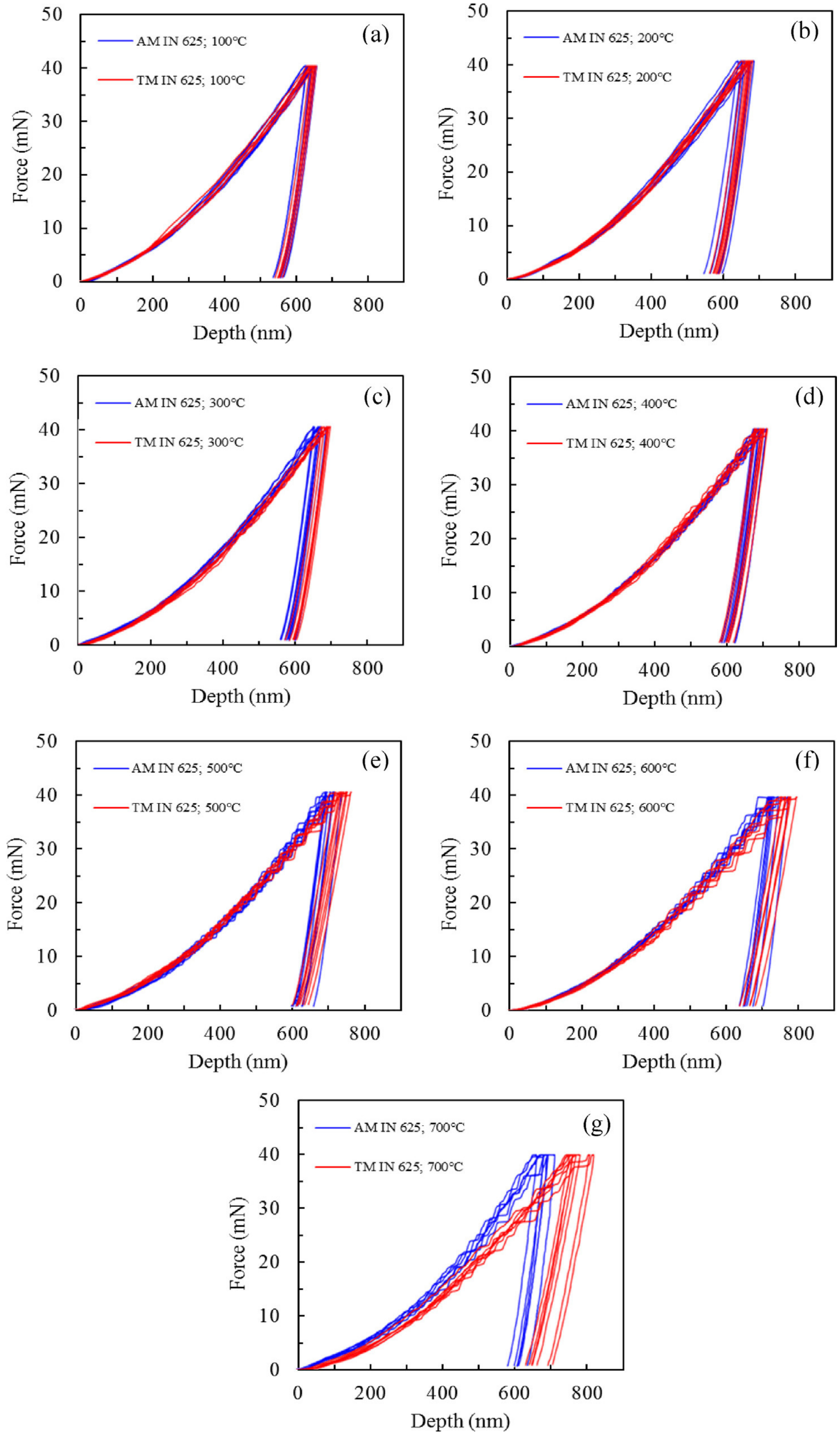

Fig. 1. Representative nanoindentation load-displacement curves for AM and TM IN 625 at several temperatures.

ferent than its wrought counter parts [16]. In addition, small scale and contact creep might deviate from unidirectional testing [17]. AM IN 625 is a promising candidate to be utilized for several high temperature applications, including joints, contacts, and interfaces. Furthermore, recently advanced nanoindenters have become highly capable of capturing mechanical properties and creep. Yet, to the best of authors' knowledge, elevated temperature creep

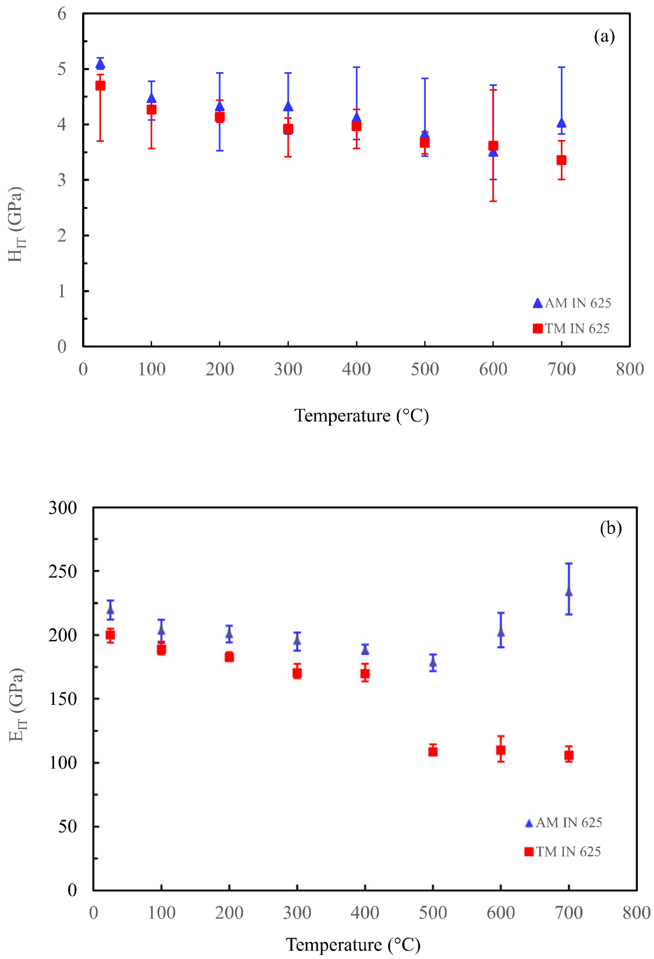

Fig. 2. Comparison of AM and TM mechanical properties (a) indentation hardness, (b) elastic modulus.

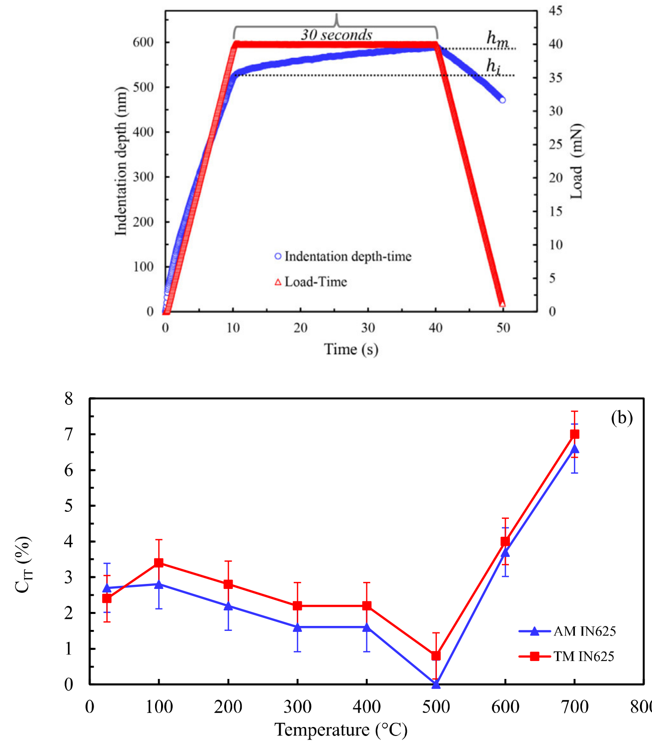

Fig. 3. Nanoindentation creep properties; (a) typical load-displacement curve, (b) C_{IT} plot of IN 625 against temperature.

deformation of AM IN 625 through nanoindentation has not been studied.

The current work investigates and compares the mechanical and creep behaviors of AM and TM IN 625 in a temperature range of room temperature (RT) to 700 °C using instrumented nanoindentation. The properties measured are elastic modulus, indentation hardness, and creep indentation depth.

2. Results and discussions

2.1. High temperature nanoindentation

Fig. 1 represents indentation load vs. displacement curves for the AM and TM IN 625 specimens. It is observed that by increasing the temperature, the serrations on both AM and TM specimens increase. The presence of the serration in the force-displacement graph is mainly due to the dynamic strain aging (DSA) which is typical for nickel-based alloys [10].

2.2. Indentation hardness and elastic modulus

Fig. 2(a) shows the indentation hardness (H_{IT}) variation with the temperature for AM and TM IN 625 specimens. The indentation hardness of both specimens generally shows a slight decrease with the temperature that expected to be due to the thermal softening [18]. The higher nanoindentation hardness for AM specimens is attributed to the availability of large amounts of (geometrically necessary dislocations) GNDs which are inherently associated with the AM manufacturing process [14]. GNDs prevent slip, and consequently raise yield strength and hardness [19]. As the temperature increases, hardness values monotonically decrease for the TM specimens. For the AM specimens, the hardness decreases when the temperature increases from RT to 600 °C (5.2 GPa to about 3.5 GPa), and it goes back up slightly to about 4.2 GPa at 700 °C. The observed increase in the hardness with temperature at 700 °C can be attributed to a thermally activated cross-slip of dislocations requiring cross slip of screw segments in order for the dislocation to bypass the precipitate obstacles, and the locking of screw segments of the two coupled partial dislocations [20]. In AM samples, the hardening via GNDs overshadows the softening via thermal softening and hence, the overall net outcome is hardening. The hardness values measured here are in the range of what was reported by Zhang et al. [18].

Fig. 2(b) shows the measured elastic modulus of AM and TM IN 625 specimens at different temperatures. The room temperature elastic modulus of the TM IN 625 specimen was measured to be 218 GPa. This is, indeed, close to the reported values from the tensile test at the macroscale [18]. As shown in Fig. 2(b), the elastic modulus of TM IN 625 specimen drops significantly with increasing temperature to 500 °C, yet it remains fairly constant afterward. For AM specimen, the elastic modulus decreases with elevating the temperature to 500 °C but then it increases at higher temperatures and goes even above the elastic modulus value at RT. Considering the TTT diagram for IN 625, one can conclude that the presence of Nb in IN 625 leads to the formation of needle-like Ni_3Nb (γ'') phase in the temperature range of 600 °C to 750 °C [9]. The formation of the precipitates probably happened during the waiting time (~3 h) for the thermal stability of the tip and the specimen as well as their thermal equilibrium before conducting the measurements. Hence, the increased elastic modulus at 600 and 700 °C for AM sample and the observed constant elastic modulus at the same range of temperature for TM sample can be attributed to the early precipitation of this metastable phase in AM specimens. Additional investigation and experimentation, in particular transmission electron microscopy, are needed to fully comprehend and explain the observed results here. These are currently being conducted by the authors and the results will be presented in the future work.

2.3. High temperature creep analyses

From the temporal load-displacement data, a typical creep depth profile was extracted (Fig. 3(a)). In order to quantify the creep deformation, a normalized and simple isothermal creep index (C_{IT}) is defined as:

$$C_{IT} = \frac{h_m - h_i}{h_m} \quad (1)$$

where h_m is the maximum indentation depth at the end of the hold and h_i is the indentation depth at the beginning of the hold. In Fig. 3 (b), the C_{IT} value for AM and TM IN 625 was measured to be 2.7 and 2.4, respectively, at 100 °C. The C_{IT} curves obtained from the specimens follow a similar trend while C_{IT} values of AM specimen are less than C_{IT} of TM curve at elevated temperatures. Through conventional creep test, Son et al. [9] found that the amount of γ'' and δ participates was higher in AM IN 625 than TM sample in both 650 and 800 °C resulting in the alloy strengthening and reduction in creep. As can be seen in Fig. 3(b), while both specimen types show the lowest C_{IT} at 500 °C, a closer look reveals that at 500 °C, the C_{IT} index for AM specimen is almost zero and no change in the indentation depth of the material occurs after 30 s. Such a property is typically caused by the hardening precipitates, which act as obstacles during dislocation motion. However, additional transmission electron microscopy is needed to be conducted to evaluate the validity of this point. The C_{IT} values for both AM and TM IN 625 severely increased at 600 and 700 °C. Higher temperatures tend to drive the dislocation past obstacles and barriers and result in creep deformation.

3. Conclusion

In the current study, the indentation hardness, elastic modulus and creep properties of both AM IN 625 and TM IN 625 specimens were studied at RT, 100, 200, 300, 400, 500, 600, and 700 °C through high temperature nanoindentation method. Results showed that the indentation hardness of both IN 625 specimens decreases as the temperature increases up to 600 °C, nonetheless, for AM IN 625 it increases slightly at 700 °C. It was found that the AM IN 625 specimen has a better creep resistance at elevated temperatures and especially at 500 °C than the TM specimen.

Declaration of Competing Interest

The authors declare that they have no known competing financial interests or personal relationships that could have appeared to influence the work reported in this paper.

Acknowledgments

Keivan Davami acknowledges the support of the Advanced Manufacturing program of the National Science Foundation, award CMMI-AM #2029059. The support of Anton Paar In. is acknowledged.

Appendix A. Supplementary data

Supplementary data to this article can be found online at https://doi.org/10.1016/j.mfglet.2022.05.001.

References

[1] L. Lu, Y. Tian, Y. Cai, Y. Xin, X. Chen, G. Zhang, J. Han. Microstructure and mechanical properties of a functionally graded material from TA1 to Inconel 625 fabricated by dual wire + arc additive manufacturing Mater Lett. 298. (2021). . 130010, 10.1016/j.matlet.2021.130010.
[2] Sohrabian M, Vaseghi M, Khaleghi H, Dehrooyeh S, Afshar Kohan MS. Structural Investigation of Delicate-Geometry Fused Deposition Modeling Additive Manufacturing Scaffolds: Experiment and Analytics. J Mater Eng Perform 2021;30:6529–41. https://doi.org/10.1007/s11665-021-05894-y.
[3] J.J. Lewandowski, M. Seifi Metal Additive Manufacturing: A Review of Mechanical Properties Annu Rev Mater Res, 46 (2016), pp. 151–186, 10.1146/annurev-matsci-070115-032024.
[4] A.W. Gebisa, H.G. Lemu Additive Manufacturing for the Manufacture of Gas Turbine Engine Components: Literature Review and Future Perspectives Proceedings of ASME Turbo Expo 2018 Turbomachinery, June (2018), Oslo, Norway, 10.1115/GT2018-76686.
[5] Ning J, Sievers DE, Garmestani H, Liang SY. Analytical Modeling of In-Process Temperature in Powder Bed Additive Manufacturing Considering Laser Power Absorption, Latent Heat. Scanning Strategy, and Powder Packing Mater 2019;12(5):808. https://doi.org/10.3390/ma12050808.
[6] Criales LE, Arısoy YM, Lane B, Moylan S, Donmez A, Özel T. Predictive modeling and optimization of multi-track processing for laser powder bed fusion of nickel alloy 625. Addit Manuf 2017;13:14–36.
[7] Arısoy YM, Criales LE, Özel T, Lane B, Moylan S, Donmez A. Influence of scan strategy and process parameters on microstructure and its optimization in additively manufactured nickel alloy 625 via laser powder bed fusion. Int J Adv Manuf Technol 2017;90:1393–417. https://doi.org/10.1007/s00170-016-9429-z.
[8] S. Wu, H.Y. Song, H.Z. Peng, P.D. Hodgson, H. Wang, X.H. Wu, Y.M. Zhu, M.C. Lam, A.J. Huang A microstructure-based creep model for additively manufactured nickel-based superalloys Acta Materialia, 224 (2022), p. 117528, 10.1016/j.actamat.2021.117528.
[9] K. Son, M.E. Kassner, K.A. Lee The Creep Behavior of Additively Manufactured Inconel 625 Adv Eng Mater, 22 (2020), p. 1900543, 10.1002/adem.201900543.
[10] R.A. Rowe, A. Tajyar, M. Munther, K.E. Johanns, P.G. Allison, K. Momeni, K. Davami Nanoscale serration characteristics of additively manufactured superalloys J Alloys Compd, 854 (2021), p. 156723, 10.1016/j.jallcom.2020.156723.
[11] Zhang Y, Mohanty DP, Seiler P, Siegmund T, Kruzic JJ, Tomar V. High temperature indentation based property measurements of IN-617. Int J Plast 2017;96:264–81. https://doi.org/10.1016/j.ijplas.2017.05.007.
[12] S. Salari, M.d.S. Rahman, A.A. Polycarpou, A. Beheshti Elevated temperature mechanical properties of Inconel 617 surface oxide using nanoindentation Mater Sci Eng A, 788 (2020), p. 139539, 10.1016/j.msea.2020.139539.
[13] A. Sawant, S. Tin, J.-C. Zhao High Temperature Nanoindentation of Ni-base Superalloys In: R.C. Reed, K.A. Green, P. Caron, T. Gabb, M.G. Fahrmann, E.S. Huron, S.A. Woodard (eds) Superalloys (2008) TMS, pp. 863–871, doi: 10.7449/2008/superalloys_2008_863_871.
[14] H. Wang, A. Dhiman, H.E. Ostergaard, Y. Zhang, T. Siegmund, J.J. Kruzic, V. Tomar Nanoindentation based properties of Inconel 718 at elevated temperatures: A comparison of conventional versus additively manufactured samples Int J Plast, 120 (2019), pp. 380–394, 10.1016/j.ijplas.2019.04.018.
[15] M. Tripathy, M. Munther, K. Davami, A. Beheshti Surface property study of additively manufactured Inconel 625 at room temperature and 510 °C Manuf Lett, 26 (2020), pp. 69–73, 10.1016/j.mfglet.2020.10.001.
[16] K.T. Son, M.E. Kassner, K. A. Lee The Creep Behavior of Additively Manufactured Inconel 625 Adv Eng Mater, 22 (2020), p. 1900543, 10.1002/adem.201900543.
[17] S. Sepehr, A. Beheshti Asperity-based contact and static friction with provision for creep: A review Surf Interfaces, 24 (2021), p. 101144, 10.1016/j.surfin.2021.101144.
[18] Y.C. Zhang, X.T. Yu, W. Jiang, S.T. Tu, X.C. Zhang Elastic modulus and hardness characterization for microregion of Inconel 625/BNi-2 vacuum brazed joint by high temperature nanoindentation Vacuum, 181 (2020), p. 109582, 10.1016/j.vacuum.2020.109582.
[19] N.A. Fleck, M.F. Ashby, J.W. Hutchinson The role of geometrically necessary dislocations in giving material strengthening Scr Mater, 48 (2003), pp. 179–183, 10.1016/S1359-6462(02)00338-X.
[20] P. Pandey, A. Sawant, N. Baler, S.K. Makineni, K. Chattopadhyay Effect of Ru addition on γ/γ' microstructural stability in a low-density CoNi based superalloy Scr Mater, 208 (2022), p. 114318, 10.1016/j.scriptamat.2021.114318.